Journal of Materials Chemistry

Cite this: J. Mater. Chem., 2011, 21, 19058

www.rsc.org/materials

PAPER

# A weak electron transporting material with high triplet energy and thermal stability *via* a super twisted structure for high efficient blue electrophosphorescent devices†

**Lixin Xiao,*[a] Boyuan Qi,[a] Xing Xing,[a] Lingling Zheng,[a] Sheng Kong,[a] Zhijian Chen,[a] Bo Qu,[a] Lipei Zhang,[a] Ziwu Ji[b] and Qihuang Gong*[a]**

*Received 22nd July 2011, Accepted 22nd September 2011*
**DOI: 10.1039/c1jm13488d**

A high triplet energy ($E_T$ = 3.2 eV) electron transporting/hole blocking (ET/HB) material, 1,2,4,5-tetra (3-pyrid-3-yl-phenyl)benzene (TemPPB) with a super twisted structure and high thermal stability has been synthesized. An external quantum efficiency (EQE) of 19.6% was achieved by using TemPPB as the ET/HB material in a blue electrophosphorescent device, much higher than the EQE of 12.5% for the device using the conventional ET material, 3-(4-biphenyl)-4-phenyl-5-(4-*tert*-butylphenyl)-1,2,4-triazole (TAZ). In addition, the weak ET property of TemPPB resulting from its super twisted structure can be enhanced *via* n-type doping with LiF. An EQE of 24.5% was achieved by combining n-type doping and a double-emission layer. This shows an alternative way to design ET/HB materials with high $E_T$ and improved thermal stability for blue electrophosphorescent devices.



## Introduction

For both displays and solid state lighting, efficiency is still the crucial factor in the application of organic light-emitting devices (OLEDs). Thus the full use of singlet and triplet excitons, electrophosphorescence, has attracted increasing attention since it was first reported.[1–3] The use of phosphorescent emitters is one of the most important strategies to improve the efficiency of OLEDs. Despite great achievements in red and green phosphorescent materials, improving efficiency for blue emission seems to be the final obstacle for commercialization of full color displays and white light application.

Generally, the hole mobility is much higher (about 1000 times) than the electron mobility in organic semiconducting materials,[4] and thus holes are much easier to transport than electrons in phosphorescent OLEDs (PhOLEDs). Therefore, the development of efficient electron transporting/hole blocking (ET/HB) materials is crucial to improving the efficiency of PhOLEDs. Although several traditional ET/HB compounds have been used in blue electrophosphorescence, high efficiency cannot be achieved because their triplet energy ($E_T$) is lower than that of the blue emitter iridium(III) bis[(4,6-difluorophenyl)-pyridinato-*N*,$C^{2'}$]picolinate (FIrpic), and triplet excitons and/or holes cannot be confined within the emissive layer.

A high $E_T$ may be obtained if the π-conjugation system is blocked. Two ways can be used to achieve this, one of which is to introduce a central atom connection. By introducing phenyl or boron as the central group, Kido and his co-workers developed a series of ET/HB materials with high $E_T$, *e.g.* 1,3,5-tri(*p*-pyrid-3-yl-phenyl)benzene (TpPyPB),[5] 1,3,5-tri(*m*-pyrid-3-yl-phenyl) benzene (TmPyPB),[5] 3,3″,5,5″-tetra(3-pyridyl)-1,1′;3′,1″-terphenyl (B3PyPB),[6] and tris[3-(3-pyridyl)mesityl]borane (3TPYMB)[7,8] and achieved external quantum efficiencies (EQEs) of over 20% for blue PhOLEDs. Introducing a phosphine oxide (P=O) group is also possible to weaken the molecular conjugation; derivatives with high $E_T$ as effective bipolar hosts and ET/HB materials for blue PhOLEDs have been reported.[9–14]

We previously prepared a weak ET material, diphenyl-bis[4-(pyridin-3-yl)phenyl]silane (DPPS) by using a silicon atom as the central group to weaken the conjugation,[15] with effective HB property and high $E_T$ with effective exciton blocking (EB) property to achieve nearly a 100% internal quantum efficiency (IQE) in a FIrpic-based device. Therefore, ET/HB materials with higher $E_T$ and large enough ion potential ($I_p$) compared to those of phosphorescent dyes are crucial to improving the efficiency of blue PhOLEDs.[16]

Based on the results above, inserting a central atom, *e.g.* silicon ($E_T$ = 2.7–3.3 eV),[10,16] boron ($E_T$ = 3.0 eV)[7,8] or P=O ($E_T$ = 3.3 eV)[10] to weaken the π-conjugation is an effective way to achieve high $E_T$. However, the central atom connection led to poorer thermal stability, and hence further improvements are still needed. If the central atom was replaced by a phenyl group as

[a]*State Key Laboratory for Mesoscopic Physics and Department of Physics, Peking University, Beijing, 100871, P. R. China. E-mail: lxxiao@pku.edu.cn; qhgong@pku.edu.cn*
[b]*School of Physics, Shandong University, Jinan, 250100, P. R. China*
† Electronic supplementary information (ESI) available: TOF measurement and low temperature photoluminescence spectrum. See DOI: 10.1039/c1jm13488d

mentioned above, although this could improve the thermal properties, it would be difficult to further increase the $E_T$ (2.6–2.8 eV)[5,6] because of their near coplanarity originating from their lower steric hindrance. For example, the $E_T$ of the 3,5-dipyridylphenyl derivative of B3PyPB is 2.77 eV, although it shows a glass-transition temperature ($T_g$) of 106 °C (Table 1).[6]

In this paper, we report a second way to achieve high $E_T$ by using a super twisted structure and meta-position[17] linking to block the π-conjugation. We synthesize an ET/HB material, 1,2,4,5-tetra(3-pyrid-3-yl-phenyl)benzene (TemPPB), which exhibits a super twisted structure originating from steric hindrance. This conformation suppresses the electron delocalization and results in a wide $E_g$ and high $E_T$. The molecular conformation of TemPPB optimized by Gaussian 09 (Hartree–Fock method, at the 6-31G* level) is shown in Fig. 1. The distance between the upper and the lower groups is calculated to be 9.18 Å, which indicates that the molecular conformation is far from coplanar. The super twisted structure is beneficial to the suppression of aggregation in the film state and to the $T_g$ which is 97 °C, much higher than the 50 °C for DPPS (with Si as the central atom). These may increase the stability of the device. When it was employed in a blue PhOLED as the combined ET/HB layer, an EQE of 19.6% was achieved which was increased to 24.5% by combination with n-type doping and a double-emission layer. This suggests an alternative way to design ET/HB materials with high $E_T$ and improved thermal stability for blue electrophosphorescent devices.

## Results and discussion

The synthetic route of TemPPB is shown in Scheme 1. 3-bromopyridine was reacted with 3-chlorophenyl boronic acid *via* a Suzuki cross-coupling reaction[18] to yield **1**, followed by boronation to afford **2** according to the literature,[19] then reacted with 1,2,4,5-tetrabromobenzene *via* a second Suzuki cross-coupling reaction. Finally a white powder of TemPPB was obtained and purified *via* sublimation before further use. The absorption and photoluminescence (PL) spectra of TemPPB, shown in Fig. 2, were measured in both the film and in tetrahydrofuran (THF) solution ($1 \times 10^{-5}$ M) at room temperature. The TemPPB film was deposited under vacuum on a quartz substrate. The absorption maximum of the TemPPB film (263 nm) is red-shifted 7 nm relative to the solution (256 nm). The peaks can be attributed to the π–π* transition. The energy gap ($E_g$) of TemPPB can be calculated from the absorption edge to be 4.0 eV, which is wider than most previously reported ET materials. The PL spectra show the peaks for the solution and film at 382 nm and 384 nm, respectively. The slight difference indicates that TemPPB tends not to aggregate in the solid state as a result of its

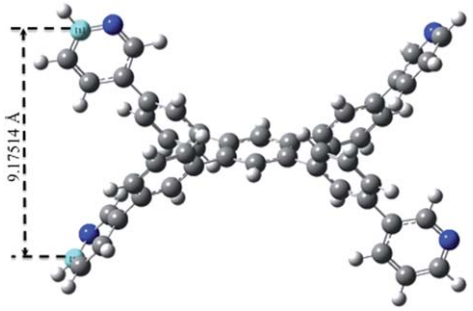


**Fig. 1** Molecular conformation of TemPPB optimized by Gaussian 09 (Hartree–Fock method, at the 6-31G* level).

super twisted structure. The lowest unoccupied molecular orbital (LUMO) level was estimated to be 3.0 eV, as measured by cyclic voltammetry (CV) with a three-electrode configuration as shown in Fig. S1.† The highest occupied molecular orbital (HOMO) level of TemPPB could be calculated from its LUMO level and $E_g$ as 7.0 eV which is low enough to block holes escaping from the emitting material (EM) layer. The low temperature phosphorescence spectrum was measured in a frozen solution (2-methyl THF) in liquid $N_2$ with a phosphorescence mode. The phosphorescence spectrum is shown in Fig. S2.† The triplet energy is calculated from the onset of the phosphorescence spectrum as B3PyPB reported by Kido.[6] The onset of phosphorescence of TemPPB is 390 nm, and accordingly the $E_T$ energy of TemPPB was calculated to be around 3.2 eV which is higher than the 2.7 eV for 3-(4-biphenyl)-4-phenyl-5-(4-*tert*-butylphenyl)-1,2,4-triazole (TAZ), a conventional ET material in PhOLEDs. The electron mobility of TemPPB was $3 \times 10^{-7}$ cm$^2$ V$^{-1}$ s$^{-1}$ measured using the time-of-flight (TOF) method (Fig. S3†). The low electron mobility of TemPPB might be due to the super twisted structure.

The thermal properties of TemPPB were measured by thermogravimetric analysis (TGA) and differential scanning calorimetry (DSC), which showed a thermal-decomposition temperature ($T_d$) at 400 °C and a $T_g$ at 97 °C. As comparison, the physical properties of materials including B3PyPB and DPPS are summarized in Table 1.

To investigate the ET/HB property of TemPPB, multilayered electrophosphorescent devices were fabricated. A glass substrate precoated with an indium tin oxide (ITO) layer was treated as in our previous report.[23] A 20 nm layer of 4,4′-bis[*N*-(*p*-tolyl)-*N*-phenyl-amino]biphenyl (TPD) or 1,1-bis[(di-4-tolylamino) phenyl]cyclohexane (TAPC) was spin coated as the hole injecting/transporting layer. 4,4′,4″-tris-(*N*-carbazolyl)-triphenylamine (TCTA) was used as the hole transporting/host layer,

**Table 1** Physical properties of the materials used

| Materials | $T_g$ (°C) | $E_a$ (eV) | $I_p$ (eV) | $E_g$ (eV) | $E_T$ (eV) | Reference |
|---|---|---|---|---|---|---|
| TemPPB | 97 | 3.0 | 7.0 | 4.0 | 3.2 | This work |
| B3PyPB | 106 | 2.62 | 6.67 | 4.05 | 2.77 | 6 |
| DPPS | 50 | 2.5 | 6.5 | 4.0 | 2.7 | 16 |
| TAZ | 70 | 2.7 | 6.3 | 3.6 | 2.7 | 20,21 |
| FIrpic | | 3.5 | 6.2 | 2.7 | 2.7 | 22 |

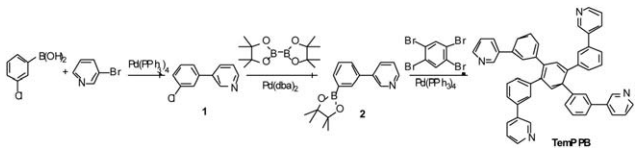


**Scheme 1** Synthetic route for TemPPB.

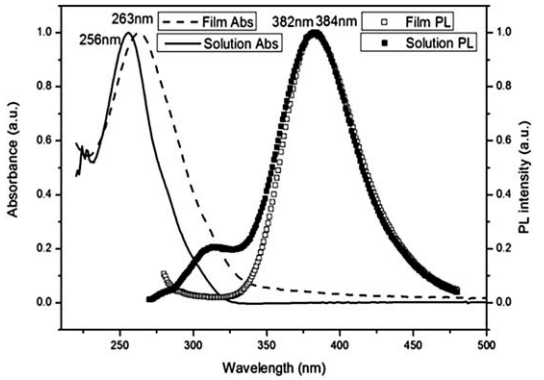


**Fig. 2** Absorption and PL spectra of TemPPB in THF ($1 \times 10^{-5}$ M) and as a film.

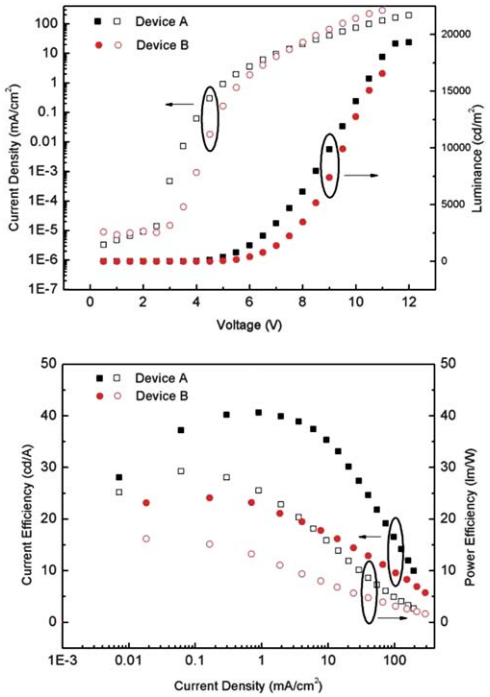


**Fig. 3** Current density and luminance–voltage and CE and PE–current density of device **A**: ITO/TPD 20 nm/TCTA 20 nm/mCP: 8%FIrpic 20 nm/TemPPB 30 nm/LiF/Al (□ ■) and **B**: ITO/TPD 20 nm/TCTA 20 nm/mCP: 8%FIrpic 20 nm/TAZ 30 nm/LiF/Al (○ ●).

FIrpic as the blue phosphorescent dye, *N*,*N*′-dicarbazolyl-3,5-benzene (mCP) as the host, TemPPB or TAZ (reference device) as the ET layer, LiF as the electron injection layer and Al as the cathode. The structures of the devices fabricated are shown in the following.

Device **A**: ITO/TPD 20 nm/TCTA 20 nm/mCP: 8%FIrpic 20 nm/TemPPB 30 nm/LiF/Al

Device **B**: ITO/TPD 20 nm/TCTA 20 nm/mCP: 8%FIrpic 20 nm/TAZ 30 nm/LiF/Al

Device **C**: ITO/TPD 20 nm/TCTA 20 nm/mCP: 8%FIrpic 20 nm/TemPPB: 1%LiF 30 nm/LiF/Al

Device **D**: ITO/TPD 20 nm/TCTA 20 nm/mCP: 8%FIrpic 20 nm/TemPPB 10 nm/TemPPB: 1%LiF 20 nm/LiF/Al

Device **E**: ITO/TAPC 20 nm/TCTA: 8%FIrpic 20 nm/mCP: 15%FIrpic 20 nm/TemPPB 10 nm/TemPPB: 1%LiF 20 nm/LiF/Al

The current density and luminance–voltage characteristics of devices **A** and **B** are shown in Fig. 3. The current density of device **A** is slightly higher than that of the device **B** and the turn-on voltages (at 1 cd $m^{-2}$) are 3.4 V and 4.3 V for devices **A** and **B**, respectively, although the electron mobility of TemPPB is $3 \times 10^{-7}$ $cm^2$ $V^{-1}$ $s^{-1}$, slightly lower than the $\sim 10^{-6}$ $cm^2$ $V^{-1}$ $s^{-1}$ for TAZ.[6] This might be due to the pyridine component which enhanced electron injection/transportation between the metal electrode and organic layer.[24]

Moreover, device **A** achieves a maximum luminance of 19300 cd $m^{-2}$, a maximum current efficiency (CE) of 40.6 cd $A^{-1}$ and a maximum power efficiency (PE) of 29.2 lm $W^{-1}$ corresponding to an EQE of 19.6%, while device **B** shows a maximum luminance of 16540 cd $m^{-2}$, a maximum CE of 24.1 cd $A^{-1}$ and a maximum PE of 16.1 lm $W^{-1}$ corresponding to an EQE of 12.5% (Table 2).

The higher $E_T$ for TemPPB (3.2 eV compared to 2.7 eV for TAZ) may be the major reason for the greatly enhanced performance, because the triplet excitons are expected to be more effectively confined within the EM layer by TemPPB than TAZ. In addition, since organic materials are normally better p-type than n-type conductors, the mobilities of holes are expected to be higher than those of electrons in the device. Because of the wider $E_g$, *i.e.*, the HOMO energy or $I_p$ is deeper than that of TAZ, the holes within the EM layer in device **A** can be more effectively blocked than in device **B**.

The super twisted structure results in not only a high $E_T$, but also low electron mobility for TemPPB because it is far from coplanar. To enhance the ET property in a device, we doped TemPPB with 1% LiF; the current density of the device increased compared with the undoped ET layer (Fig. 4). Similar enhancements in current density were also previously reported for tris(8-hydroxyquinolato)aluminium ($Alq_3$) upon doping with LiF[25] and MnO.[26] When the whole 30 nm ET layer was doped with 1% LiF (device **C**), the current density was greatly enhanced (Fig. 4). However, the efficiency of device **C** with doping was lower than that of device **A** without doping. This might be attributed to exciton quenching induced by doping, because the efficiency

**Table 2** Performance of the devices

| Device | $V_{on}$ (V) | $L_{max}$ (cd $m^{-2}$) | $CE_{max}$ (cd $A^{-1}$) | $PE_{max}$ (lm $W^{-1}$) | EQE (%) |
|---|---|---|---|---|---|
| **A** | 3.4 | 19300 | 40.6 | 29.2 | 19.6 |
| **B** | 4.3 | 16540 | 24.1 | 16.1 | 12.5 |
| **C** | 3.1 | 16000 | 19.9 | 19.6 | 8.0 |
| **D** | 3.2 | 17440 | 33.0 | 32.4 | 11.9 |
| **E** | 4.1 | 22680 | 52.2 | 38.5 | 24.5 |

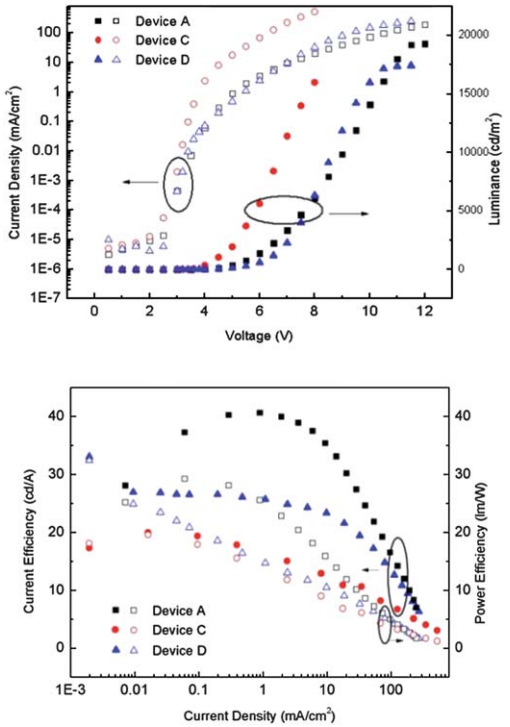


**Fig. 4** Current density and luminance–voltage and CE and PE–current density of device **A**: ITO/TPD 20 nm/TCTA 20 nm/mCP: 8%FIrpic 20 nm/TemPPB 30 nm/LiF/Al (□ ■), **C**: ITO/TPD 20 nm/TCTA 20 nm/mCP: 8%FIrpic 20 nm/TemPPB: 1%LiF 30 nm/LiF/Al (○ ●) and **D**: ITO/TPD 20 nm/TCTA 20 nm/mCP: 8%FIrpic 20 nm/TemPPB 10 nm/TemPPB: 1%LiF 20 nm/LiF/Al (△ ▲).

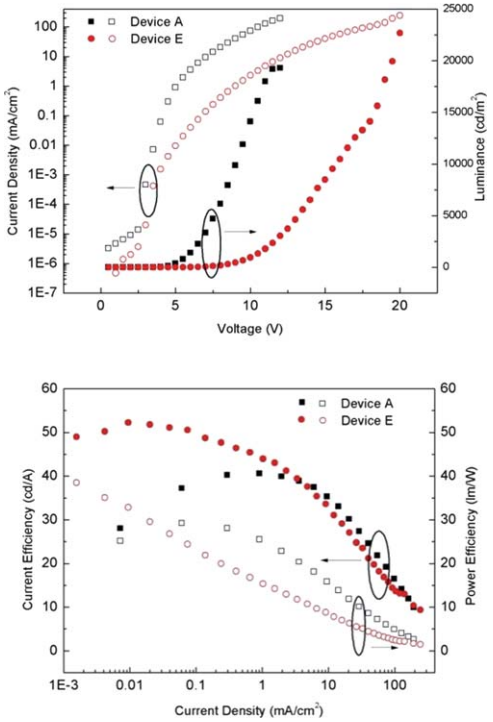


**Fig. 5** Current density and luminance–voltage and CE and PE–current density of device **A**: ITO/TPD 20 nm/TCTA 20 nm/mCP: 8%FIrpic 20 nm/TemPPB 30 nm/LiF/Al (□ ■) and **E**: ITO/TAPC 20 nm/TCTA: 8% FIrpic 20 nm/mCP: 15%FIrpic 20 nm/TemPPB 10 nm/TemPPB: 1%LiF 20 nm/LiF/Al (○ ●).

decreased with increasing thickness of the doped ET layer. When only 20 nm of the whole ET layer (30 nm) was doped with 1% LiF (device **D**), the current density decreased compared to that of device **C**, but was still higher than that of device **A** without doping. Moreover the PE of device **D** is also higher than that of device **A**, which indicates that the quenching of the excitons was effectively suppressed by inserting 10 nm of undoped TemPPB between the LiF doped layer and the emitting layer. These results indicate that the weak ET resulting from the super twisted structure could be improved by n-type doping.

To reduce the triplet–triplet annihilation, a double-emission layer was chosen and the emission region could be enlarged to the TCTA layer. In addition, to avoid the back energy transfer from the TCTA layer to the hole transporting layer, TPD with low $E_T$ (2.3 eV)[27] was replaced with TAPC ($E_T$ 2.9 eV)[27] (device **E**). As seen in Fig. 5, device **E** shows a maximum luminance over 22680 cd $m^{-2}$, a maximum CE of 52.2 cd $A^{-1}$ and a maximum PE of 38.5 lm $W^{-1}$ corresponding to an EQE of 24.5% (Table 2). The enhancement of efficiency can be attributed to the n-type doping of LiF and high $E_T$ of TAPC. However the turn-on voltage is increased to 4.1 V because the HOMO of TAPC is 5.5 eV, higher than the 5.3 eV of TPD which is closer to the work function of ITO. It is also responsible for the lower current density of device **E** compared to device **A**, because the n-type doped device showed higher current density than that of device **A**. The electroluminescence (EL) spectra of the devices are very similar and are shown in Fig. S4.†

## Conclusions

In conclusion, an ET/HB material, TemPPB, was synthesized with a super twisted structure and meta-position linking to suppress electron delocalization, leading to a wide $E_g$ (4.0 eV) and high $E_T$ (3.2 eV) originating from the steric hindrance. An EQE of 19.6% was achieved by using TemPPB as the ET/HB material for a blue electrophosphorescent device, much higher than the EQE of 12.5% for the device using the conventional ET material, TAZ. Moreover, the super twisted structure is beneficial to the suppression of aggregation in the film state and the thermal stability was also improved which may increase the stability of the device. In addition, the weak ET property of TemPPB resulting from the super twisted structure can be enhanced *via* n-type doping with LiF. An EQE of 24.5% was achieved by a combination of n-type doping and a double-emission layer. This shows an alternative way to design ET/HB materials with high $E_T$ and improved thermal stability for blue electrophosphorescent devices.

## Experimental

### General

The $^1$H NMR and $^{13}$C NMR spectra were recorded on a Bruker DPX-400 spectrometer (400 MHz). The mass spectrum was recorded on a Bruker Apex IV FTMS spectrometer. Elemental analysis was measured on an Elementar Vario MICRO CUBE (Germany). Ultraviolet-visible (UV-vis) absorption and PL

spectra were obtained on an Agilent UV-vis Spectroscopy System (8453*E*). The low temperature phosphorescence spectrum measurement was carried out on a Hitachi Fluorescence Spectrometer (F-4500) under liquid nitrogen from a frozen solution (2-methyl THF) with a phosphorescence mode. The electrochemical properties were measured in $CH_3CN$ solution containing 0.1 M of tetrabutylammonium perchlorate as the supporting electrolyte at a scanning rate of 0.1 V $s^{-1}$ by cyclic voltammetry on a CHI 650 electrochemistry workstation with a Pt disk working electrode, Pt wire counter electrode, and a saturated calomel reference electrode (SCE). Thermal properties were determined with thermogravimetric analysis (TA Instrument Q50) and differential scanning calorimetry (TA Instrument Q100).

### Synthesis of 1,2,4,5-tetra(3-pyrid-3-yl-phenyl)benzene (TemPPB)

The syntheses of 3-pyrid-3-yl chlorobenzene (**1**) and 3-(3-(4,4,5,5-tetramethyl-1,3,2-dioxaborolan-2-yl)phenyl)pyridine (**2**) were performed following the literature.[19] 1,2,4,5-tetrabromobenzene (0.67 g, 1.70 mmol), **2** (2.48 g, 15.8 mmol) were put into a three-neck flask, then toluene (60 mL), ethanol (20 mL) and 2 M aqueous potassium carbonate (20 mL) were added to it. Under nitrogen atmosphere, the mixture was stirred at 90 °C for 1 h. Then tetrakis(triphenylphosphine)palladium(0) (Pd$(PPh_3)_4$) (0.16 g, 0.1 mmol) was added to the mixture, followed by refluxing for another 24 h. After cooling down to room temperature, the mixture was poured into water and then extracted with chloroform three times. The combined organic phase was collected and dried with $MgSO_4$. The solvent was removed under reduced pressure. The residue was purified by silica-gel column chromatography with chloroform/methanol (30 : 1) as the eluent. The product (after removing the solvents) was obtained as a white solid in 82% yield (0.97 g). Finally a further purification was carried out *via* sublimation before use. $^1$H NMR ($CDCl_3$, TMS, $\delta$): 7.26–7.28 (m, 4H), 7.43–7.49 (m, 16H), 7.61–7.63 (m, 4H), 7.73 (s, 2H), 8.53–8.56 (m, 8H); $^{13}$C NMR ($CDCl_3$, TMS, $\delta$): 123.52, 125.77, 129.14, 129.20, 129.47, 132.60, 134.37, 136.35, 137.61, 139.67, 141.34, 148.04, 148.37. MS (ESI, *m*/*z*): 691.3 (calcd for $C_{50}H_{34}N_4$: 690.3). Anal. Calcd for $C_{50}H_{34}N_4$: C, 86.93; H, 4.96; N, 8.11. Found: C, 86.90; H, 4.97; N, 8.13.

### Device fabrication and characterization

An ITO-coated substrate with a sheet resistance of 10 Ω $sq^{-1}$ was used as the anode. It was cleaned with deionized water, acetone and ethanol in sequence under ultrasonication and finally treated with oxygen plasma. TPD or TAPC was dissolved in 1,2-dichloroethane, filtered through a 0.22 μm filter and spin-coated onto the surface of the ITO to act as a hole injecting/transporting layer. After that, it was loaded into a vacuum chamber and the other materials were all deposited by thermal evaporation under high vacuum ($10^{-4}$ Pa). An ultra thin layer of LiF (0.5 nm) and an aluminium layer (100 nm) were evaporated in vacuum as the cathode, the area of which was defined as the active area of the devices by a shadow mask with 2 mm diameter opening. The thickness of the evaporating layer was monitored with a quartz crystal microbalance. The device performances were measured with a Keithley 2611 source meter and a spectrophotometer (Photo Research 650). All the measurements were carried out in ambient atmosphere at room temperature.

## Acknowledgements

This work was financially supported by the National Basic Research Program of China (grants 2009CB930500 and 2007CB307000), NSFC (grants 61177020, 10934001, 60907015 and 10821062), and Beijing Municipal Science and Technology Project (Z101103050410002). The authors thank Dr Z. Chu and Prof. D. Zou of the College of Chemistry and Molecular Engineering, Peking University for the TOF measurement and Ms J. You and Prof. P. Wang of the Technical Institute of Physics and Chemistry, CAS, for the phosphorescence spectrum measurement.

## References

1 S. Hoshino and H. Suzuki, *Appl. Phys. Lett.*, 1996, **69**, 224.
2 Y. Ma, H. Zhang, J. Shen and C. Che, *Synth. Met.*, 1998, **94**, 245.
3 M. A. Baldo, D. F. O'Brien, Y. You, A. Shoustikov, S. Sibley, M. E. Thompson and S. R. Forrest, *Nature*, 1998, **395**, 151.
4 H. Antoniadis, M. A. Abkowitz and B. R. Hsieh, *Appl. Phys. Lett.*, 1994, **65**, 2030.
5 S.-J. Su, T. Chiba, T. Takeda and J. Kido, *Adv. Mater.*, 2008, **20**, 2125.
6 H. Sasabe, E. Gonmori, T. Chiba, Y.-J. Li, D. Tanaka, S.-J. Su, T. Takeda, Y.-J. Pu, K. I. Nakayama and J. Kido, *Chem. Mater.*, 2008, **20**, 5951.
7 D. Tanaka, Y. Agata, T. Takeda, S. Watanabe and J. Kido, *Jpn. J. Appl. Phys.*, 2007, **46**, L117.
8 D. Tanaka, T. Takeda, T. Chiba, S. Watanabe and J. Kido, *Chem. Lett.*, 2007, **36**, 262.
9 J. Ding, Q. Wang, L. Zhao, D. Ma, L. Wang, X. Jing and F. Wang, *J. Mater. Chem.*, 2010, **20**, 8126.
10 S. O. Jeon, S. E. Jang, H. S. Son and J. Y. Lee, *Adv. Mater.*, 2011, **23**, 1436.
11 S. O. Jeon, K. S. Yook, C. W. Joo and J. Y. Lee, *Adv. Mater.*, 2010, **22**, 1872.
12 S. O. Jeon, K. S. Yook, C. W. Joo and J. Y. Lee, *J. Mater. Chem.*, 2009, **19**, 5940.
13 M. Mamada, S. Ergun, C. Pérez-Bolívar and P. Anzenbacher, Jr, *Appl. Phys. Lett.*, 2011, **98**, 073305.
14 A. L. V. Ruden, L. Cosimbescu, E. Polikarpov, P. K. Koech, J. S. Swensen, L. Wang, J. T. Darsell and A. B. Padmaperuma, *Chem. Mater.*, 2010, **22**, 5678.
15 L. Xiao, S.-J. Su, Y. Agata, H. Lan and J. Kido, *Adv. Mater.*, 2009, **21**, 1271.
16 L. Xiao, Z. Chen, B. Qu, J. Luo, S. Kong, Q. Gong and J. Kido, *Adv. Mater.*, 2011, **23**, 926.
17 I. Avilov, P. Marsal, J.-L. Brédas and D. Beljonne, *Adv. Mater.*, 2004, **16**, 1624.
18 N. Miyaura and A. Suzuki, *Chem. Rev.*, 1995, **95**, 2457.
19 S.-J. Su, D. Tanaka, Y. J. Li, H. Sasabe, T. Takeda and J. Kido, *Org. Lett.*, 2008, **10**, 941.
20 C.-C. Wu, C.-W. Chen and T.-Y. Cho, *Appl. Phys. Lett.*, 2003, **83**, 611.
21 M.-H. Tsai, H.-W. Lin, H.-C. Su, T.-H. Ke, C.-C. Wu, F.-C. Fang, Y.-L. Liao, K.-T. Wong and C.-I. Wu, *Adv. Mater.*, 2006, **18**, 1216.
22 S. Tokito, T. Iijima, Y. Suzuri, H. Kita, T. Tsuzuki and F. Sato, *Appl. Phys. Lett.*, 2003, **83**, 569.
23 S. Kong, L. Xiao, Y. Liu, Z. Chen, B. Qu and Q. Gong, *New J. Chem.*, 2010, **34**, 1994.
24 T. Oyamada, H. Yoshizaki, H. Sasabe and C. Adachi, *Chem. Lett.*, 2004, **33**, 1034.
25 K. R. Choudhury, J.-h. Yoon and F. So, *Adv. Mater.*, 2008, **20**, 1456.
26 J. Luo, L. Xiao, Z. Chen and Q. Gong, *Appl. Phys. Lett.*, 2008, **93**, 133301.
27 J. Lee, N. Chopra, S.-H. Eom, Y. Zheng, J. Xue, F. So and J. Shi, *Appl. Phys. Lett.*, 2008, **93**, 123306.

 